AIAA 82-4293

An Algorithm for Finite Element Analysis of Partly Wrinkled Membranes

Richard K. Miller*
University of Southern California, Los Angeles, California
and
John M. Hedgepeth†
Astro Research Corporation, Carpinteria, California

Introduction

An important structural component of many large spacecraft is a tensioned membrane surface. The design of large membrane structures for minimum weight requires extremely small pretension in the membrane, which in turn results in a high likelihood of the development of wrinkled and slack regions under expected variations in thermal strains, for example.

Presented in this Note is a generalization and numerical implementation of the Stein-Hedgepeth continuum theory[1] for analysis of partly wrinkled membranes. This approach is based on experimental observations that show that, when wrinkles develop within a membrane parallel to, say, the x direction, the associated overall contraction in the y direction exceeds that predicted by the Poisson's ratio effect. The additional average normal strain in the y direction may be regarded as an "average wrinkle strain." In Ref. 1 these geometric features of wrinkling were incorporated into a Hookean material model by appropriately increasing the local effective value of Poisson's ratio in wrinkled regions. This effective value of Poisson's ratio may be determined by imposing a locally uniaxial stress state in a wrinkled region. The net result is that effective Hookean material properties become dependent upon the local state of strain. Comparisons between the predictions of this theory and experimental results for some simple configurations[1-3] show that very satisfactory results may be obtained. Although the approximate theory attempts only to identify the average wrinkle strain, and not the details of the shape of the wrinkles, it is often these overall deformations and stresses within the membrane that are of primary concern in structural design. The model presented herein is slightly generalized from that of Ref. 1 in that slack or unstressed regions may also be included in the analysis by setting the local modulus of elasticity equal to zero in such regions.

Most structurally useful membrane surfaces are curved, being of paraboloidal, spherical, conical, or similar shape. In this Note, however, attention is confined to the simpler case of planar membranes in order to focus on useful finite element algorithms for wrinkled and slack constitutive behavior.

An Algorithm for Plane Stress

In order to illustrate the numerical implementation of the generalized Stein-Hedgepeth wrinkle model, consideration will be limited to flat membranes with in-plane loading. The resulting plane stress formulation is identical to the well-known linear elastic case[4] in every respect except the stress-strain constitutive law. A numerical algorithm that retains the simplicity of form characteristic of the linear elastic case, but is consistent with the nonlinear Stein-Hedgepeth wrinkle model, may be expressed as

$$\sigma = D\epsilon \tag{1}$$

where

$$\sigma \equiv (\sigma_x, \sigma_y, \tau_{xy})^T \qquad \epsilon \equiv (\epsilon_x, \epsilon_y, \gamma_{xy})^T \tag{2}$$

D is a local "equivalent elasticity" matrix that relates stresses σ and elastic strains ϵ within a typical element. A useful algorithm for choosing the D matrix may be expressed as

$$\begin{aligned} D &= D_s \ ; && \epsilon_1 < 0 \\ &= D_w \ ; && 0 < \epsilon_1 \text{ and } \nu\epsilon_1 < -\epsilon_2 \\ &= D_T \ ; && \text{otherwise} \end{aligned} \tag{3}$$

where

$$D_s \equiv 0 \ ; \text{ slack behavior} \tag{4}$$

$$D_T \equiv \frac{E}{1-\nu^2}\begin{bmatrix} 1 & \nu & 0 \\ \nu & 1 & 0 \\ 0 & 0 & (1-\nu)/2 \end{bmatrix} ; \text{ taut behavior} \tag{5}$$

and

$$D_w \equiv \frac{E}{4}\begin{bmatrix} 2(1+P) & 0 & Q \\ 0 & 2(1-P) & Q \\ Q & Q & 1 \end{bmatrix} ; \begin{matrix}\text{wrinkled} \\ \text{behavior}\end{matrix} \tag{6}$$

where

$$P = (\epsilon_x - \epsilon_y)/(\epsilon_1 - \epsilon_2) \qquad Q = (\gamma_{xy})/(\epsilon_1 - \epsilon_2) \tag{7}$$

In Eqs. (3-7), $\epsilon_1 > \epsilon_2$ represent the principal values of the local elastic strains ϵ, ν represents Poisson's ratio, and E represents the modulus of elasticity of the membrane material.

Numerical Implementation

Since the effective local elasticity matrix D in the equivalent linear model is dependent upon the local state of strain, an iterative solution is required. The approach used in the numerical examples that follow is based on two well-known techniques. First, the final solution is approached gradually by applying the load in progressively increasing increments. Second, for each load increment an initial guess is made for the effective local elasticity matrices in each element, based on the state of strain in the previous load increment. These matrices and the increased load are then used to obtain revised estimates for the state of strain in each element. Based on the revised strain estimates, new values of effective local elasticity matrices are obtained, and the process is repeated until convergence is achieved.

An important consideration for any algorithm that depends on an iterative solution is the rate of convergence. No analytical investigation of convergence criteria and rate of convergence was undertaken, but the algorithm was found to be quite stable and efficient in each of the numerical examples that follow. Typical results for models composed of approximately 100 triangular elements and load increments large enough to produce a 10 to 20% change in average stress levels revealed that convergence was achieved in fewer than five iterations per load increment, even though 25 to 30% of

Received July 10, 1981; revision received April 16, 1982.

*Associate Professor of Civil Engineering.
†President. Fellow AIAA.

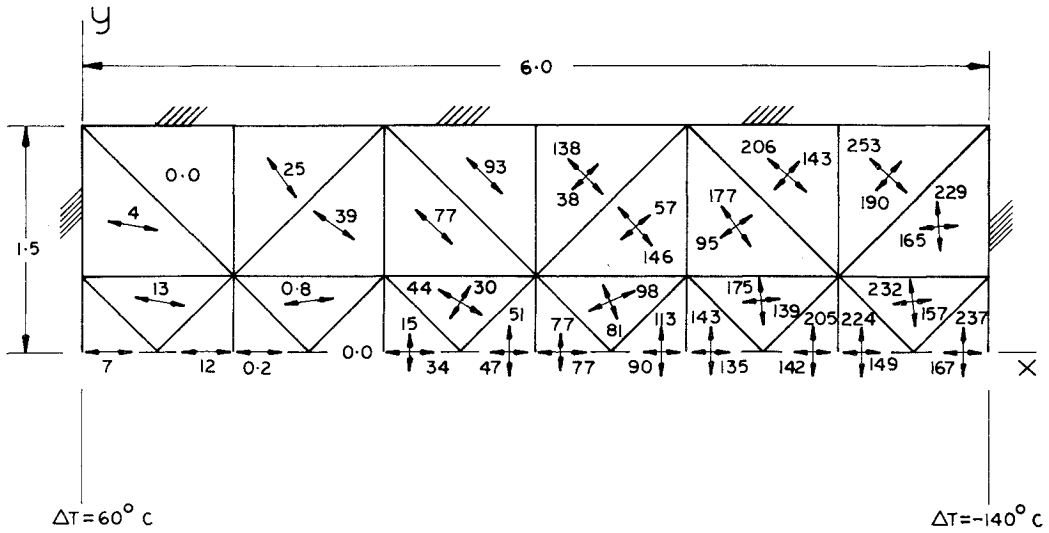

Fig. 1 Principal stresses (N/m^2) in the upper half of the grid for numerical example 1: temperature gradient. (The x axis is an axis of symmetry. Dimensions in meters.)

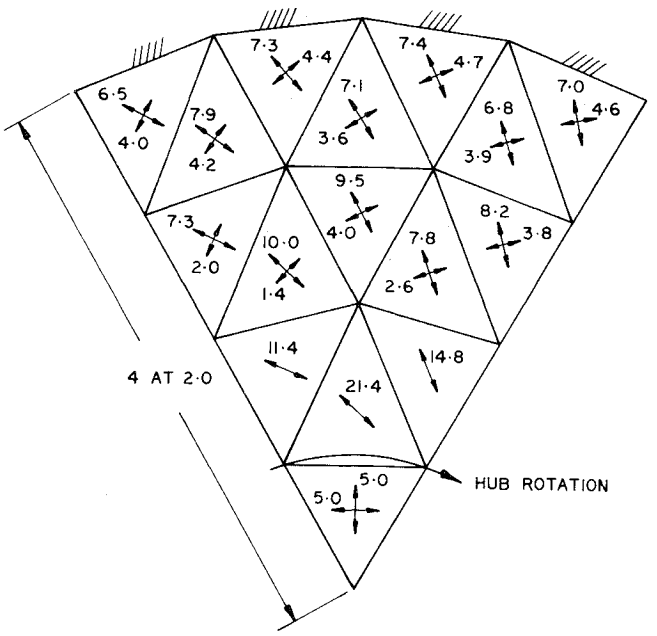

Fig. 2 Principal stresses (N/m^2) in a typical 60-deg sector of the grid for numerical example 2: hub rotation. (Dimensions in meters.)

the elements in the model contained wrinkled or slack behavior.

Illustrative Examples

As a first illustration of the nature of the results provided by the algorithm, consider a membrane attached to a rigid rectangular boundary as shown in Fig. 1. The membrane is assumed to have dimensions of 6 m×3 m, modulus of elasticity of 10^5 N/m^2, Poisson's ratio of 0.3, and coefficient of thermal expansion of $1.5\times10^{-5}/°C$. Let the membrane have no initial prestrain, but let it be subjected to a distributed change in temperature over its surface. In particular, let the temperature change vary linearly with x, ranging from a maximum of $+60°C$ at $x=0$ to a minimum of $-140°C$ at $x=6$ m. For purposes of numerical analysis, let the membrane be subdivided into 48 triangular elements with 34 nodes, as indicated in Fig. 1.

Results for the principal stresses are shown in the center of each element as orthogonally directed line segments with numerical magnitudes in N/m^2. The line segments define the orientation of the principal axes of stress. Wrinkled elements are indicated by a single line segment in a direction parallel to the wrinkles. Slack elements are indicated by the absence of any line segments and "0.0" as the magnitude of principal stress. Because of the severity of the thermal loading in this example, it is seen that 20 of the 48 elements (all in the left half of the membrane) have either developed wrinkles or gone slack. In interpreting these and all stress results presented herein, it should be noted that the stresses represent an average value over the surface of the element.

The numerical solutions for the displacements in this first example are not shown, but may be described as follows. Along the horizontal axis of symmetry of the membrane, the displacements are found to be uniaxial from left to right, with smallest magnitude near the left and right edges and largest magnitude near the center. Displacements at other nodes also tend primarily from left to right, with nodes near the left edge displaying significant motion toward the axis of symmetry and those near the right edge tending to move away from this axis.

As a second example problem, consider a membrane attached to a 24-sided (nearly circular) rigid boundary, as shown in Fig. 2. The membrane is assumed to have maximum radius of 8 m and the same material properties as in the previous example. Furthermore, let the membrane be isotropically pretensioned to a stress level of 5 N/m^2, after which a rigid hub of radius 2 m is bonded to its center. Torsional loading sufficient to develop a wrinkled region is then applied to the membrane by rotating the hub clockwise through an angle of 2.625×10^{-4} rad (0.01504 deg). For purposes of numerical analysis, let the membrane be subdivided into 96 triangular elements with 61 nodes, as indicated in the figure.

Results for the principal stresses developed in this torsion problem are again shown in the center of each element, with the same format as in the previous example. From the figure it is seen that the elements nearest the center of the membrane lie within the hub so that their isotropic stress of 5 N/m^2 is unaffected by the rigid rotation. Each element just outside but attached to the hub is found to have developed wrinkles, whereas the remainder of the elements remain taut. Note that the direction of the wrinkles is neither radial nor tangential. Nodal displacements are not shown, but they may be described as predominantly clockwise rotation, with largest magnitudes near the hub and smallest magnitudes near the outside rim.

Although the coarseness of the grid used in this example precludes quantitative comparisons, the qualitative features of these results are in agreement with those obtained experimentally and theoretically using an approximate continuum solution for similar torsion problems.[3]

The purpose of this Note is solely to demonstrate a stable algorithm for finite element analysis of partly wrinkled membranes. Questions concerning accuracy and rate of convergence in realistic technological applications are currently under investigation and will be addressed in future publications.

Acknowledgment

Funding for this research was provided by the Jet Propulsion Laboratory, California Institute of Technology, under Contract 955873.

References

[1] Stein, M. and Hedgepeth, J.M., "Analysis of Partly Wrinkled Membranes," NASA TN D-813, July 1961.

[2] Mikulas, M.M. Jr., "Behavior of Doubly Curved Partly Wrinkled Membrane Structures Formed from an Initially Flat Membrane," Ph.D. Thesis, Virginia Polytechnic Institute, Blacksburg, Va., June 1970.

[3] Mikulas, M.M. Jr., "Behavior of a Flat Stretched Membrane Wrinkled by the Rotation of an Attached Hub," NASA TN D-2456, Sept. 1964.

[4] Zienkiewicz, O.C., *The Finite Element Method*, 3rd ed., McGraw-Hill, London, 1977, pp. 93-118.

AIAA 82-4294

Load-Frequency Relations for a Clamped Shallow Circular Arch

Eric R. Johnson*
Virginia Polytechnic Institute and State University, Blacksburg, Virginia

Introduction

THE subject of this Note is the infinitesimal free vibration of a shallow circular arch about a nonlinear, prebuckled, static equilibrium configuration. The arch is elastic, its ends are clamped a fixed distance apart, and its motion is assumed to occur in its plane of curvature. It is subjected to a spatially uniform static load which can cause snap through to an inverted configuration. On a load-deflection equilibrium path, snap-through instability occurs either at a limit point (relative maximum load) or at a bifurcation point (intersection of equilibrium paths).

The results are presented as characteristic curves that are plots of the static load magnitude vs the square of the frequencies. The curve corresponding to the lowest frequency is called the fundamental characteristic curve. This curve intersects the frequency (squared) axis at the fundamental natural frequency, and intersects the load axis (zero frequency) at the snap-through load. For the arch problem considered here, the fundamental characteristic curve is concave toward the origin. This property is useful in estimating the fundamental natural frequencies, and in approximating the snap-through load experimentally but nondestructively. If the snap-through load and the fundamental natural frequency at zero load are known, then a straight line connecting these points in the characteristic plane provides a lower bound to the fundamental natural frequencies at intermediate load levels. If the fundamental natural frequencies are determined experimentally at two static load magnitudes, these results may be used to construct a straight line extrapolation to the load axis (zero frequency). This load is an upper bound to the snap-through load.

This Note is a summary of a report by the author and R. H. Plaut,[1] and is a supplement to Ref. 2 on the load-frequency relations for three shallow elastic structures, one of which is a pinned-end circular arch subject to a uniform load. Many authors have considered the free vibrations of columns, plates, and shells (see the bibliographies in Refs. 3 and 4). Fewer papers exist for shallow elastic structures.

Analysis

The shallow arch shown in Fig. 1 is homogeneous and has a uniform cross section. The unloaded configuration (dashed-dotted line) is denoted $Y_0(X)$, the equilibrium configuration under the distributed load $Q(X)$ is $Y_s(X)$, and the configuration at time T is $Y(X,T)$. Also, μ denotes the mass per unit length, E Young's modulus, I the moment of inertia of the cross section, and A the cross-sectional area.

Define the nondimensional quantities

$$x=\frac{X}{L},\quad y=\frac{Y}{2}\sqrt{\frac{A}{I}},\quad y_0=\frac{Y_0}{2}\sqrt{\frac{A}{I}},\quad y_s=\frac{Y_s}{2}\sqrt{\frac{A}{I}}$$

$$t=\pi^2 T\sqrt{\frac{EI}{\mu L^4}},\quad q=\frac{QL^4}{2\pi^4 EI}\sqrt{\frac{A}{I}} \tag{1}$$

Let dots and primes denote partial differentiation with respect to t and x, respectively. The equation of motion is

$$\pi^4\ddot{y}+y''''-y_0''''+2y''\int_0^1[(y_0')^2-(y')^2]dx=-\pi^4 q \tag{2}$$

in which axial and rotatory inertia terms are neglected. Setting the time derivative term (lateral inertia) to zero in Eq. (2) reduces it to the static equilibrium equation derived in Ref. 5. The nonlinear term in Eq. (2) represents the geometric coupling between bending and axial thrust due to large deflections. In this term the definite integral is proportional to the axial thrust, which is spatially uniform since the curvature is small. The boundary conditions are

$$y=0,\quad y'=y_0'\ \text{at}\ x=0,\ 1,\ \text{and}\ t>0 \tag{3}$$

The equilibrium configuration satisfies the equation

$$y_s''''-y_0''''+\gamma^2 y_s''=-\pi^4 q \tag{4}$$

where the induced thrust is

$$\gamma^2=2\int_0^1[(y_0')^2-(y_s')^2]dx \tag{5}$$

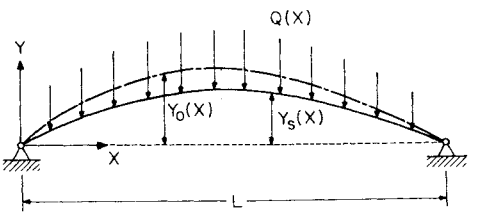

Fig. 1 Shallow arch.

Received Nov. 23, 1981; revision received March 25, 1982.

*Assistant Professor, Aerospace and Ocean Engineering. Member AIAA.